Current Medical Imaging, 2023, *19*, 1231-1244

MINI-REVIEW ARTICLE

Research on Segmentation Technology in Lung Cancer Radiotherapy Based on Deep Learning

Jun Huang[1], Tao Liu[1], Beibei Qian[1], Zhibo Chen[1] and Ya Wang[1,*]

[1]*School of Computer and Information Engineering, Fuyang Normal University, Fuyang Anhui 236037, China*

ARTICLE HISTORY

Received: May 22, 2022
Revised: November 25, 2022
Accepted: November 30, 2022

DOI:
10.2174/1573405619666230123104243

Abstract: ***Background:*** Lung cancer has the highest mortality rate among cancers. Radiation therapy (RT) is one of the most effective therapies for lung cancer. The correct segmentation of lung tumors (LTs) and organs at risk (OARs) is the cornerstone of successful RT.

Methods: We searched four databases for relevant material published in the last 10 years: Web of Science, PubMed, Science Direct, and Google Scholar. The advancement of deep learning-based segmentation technology for lung cancer radiotherapy (DSLC) research was examined from the perspectives of LTs and OARs.

Results: In this paper, Most of the dice similarity coefficient (DSC) values of LT segmentation in the surveyed literature were above 0.7, whereas the DSC indicators of OAR segmentation were all over 0.8.

Conclusion: The contribution of this review is to summarize DSLC research methods and the issues that DSLC faces are discussed, as well as possible viable solutions. The purpose of this review is to encourage collaboration among experts in lung cancer radiotherapy and DL and to promote more research into the use of DL in lung cancer radiotherapy.

Keywords: Lung cancer, deep learning, image segmentation, organs at risk, lung tumors, radiation therapy.

1. INTRODUCTION

1.1. Motivation

Lung cancer is the deadliest cancer in the world [1, 2]. Fig. (**1**) depicts WHO's global cancer data from 2020, which reveal that there were around 1.8 million fatal cases, the highest mortality rate of all cancer categories [3].

In recent years, radiation therapy (RT) has made great technological progress and has played an irreplaceable role in the treatment of lung cancer [4-8]; more than 50% of patients with malignant tumors need to receive RT [9]. The fundamental purpose of RT is to maximize the radiation dose to the target area to kill tumor cells while reducing or avoiding unnecessary radiation to the surrounding organs at risk (OARs). Therefore, the gross tumor volume (GTV), clinical target volume (CTV), and OARs should be accurately segmented in RT planning [10]. At present, automatic segmentation technology based on the atlas is more mature [11-13]; however, the biggest disadvantage of this technology is that it relies heavily on similarities between images. In recent years, several automatic segmentation techniques based on deep learning have been proposed [14-17]. Deep learning (DL) has been widely used in oncology, radiology, and other medical fields to better assist doctors with disease prediction and diagnosis [17-24]. DL in lung cancer radiotherapy segmentation can help doctors not only get more accurate and effective segmentation results [25-31], but also reduce the workload of manually segmenting patient images, allowing them to spend more time on optimizing radiotherapy plans.

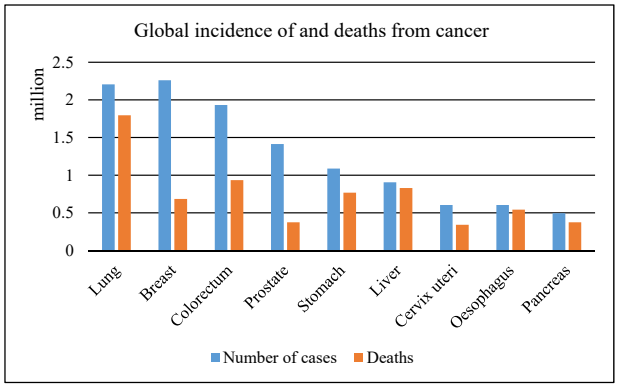

Fig. (1). Global incidence of and deaths from cancer. (*A higher resolution / colour version of this figure is available in the electronic copy of the article*).

1.2. Contribution

In this paper, we investigate the application of DL to radiotherapy in lung cancer, conduct an extensive survey of OAR and lung tumor (LT) segmentation, and compare different segmentation methods based on DL. Section 2 intro-

*Address correspondence to this author at the School of Computer and Information Engineering, Fuyang Normal University, Fuyang Anhui 236037, China; E-mail: wangya@fynu.edu.cn

duces the research strategy of the paper and some commonly used lung cancer datasets and compares this study with related work. Section 3 describes the basic knowledge and evaluation indicators of DL, and focuses on the two clinical application points of LT and OAR segmentation in the process of lung cancer radiotherapy. Section 4 discusses current challenges and possible solutions. Finally, the paper is concluded in Section 5. We investigated many pieces of literature and found that there are few reviews on deep learning-based segmentation technology for lung cancer radiotherapy (DSLC). This paper aims to present the latest developments in DSLC for researchers and provide readers with a convenient reference.

2. LITERATURE SEARCH

A large amount of literature was read during the research for this paper. This section explains the approach and selection criteria for conducting a literature search in detail. There is also a summary of commonly used lung datasets.

2.1. Search Policies and Criteria

We retrieved relevant literature from the last ten years using four databases: Web of Science, PubMed, Science Direct, and Google Scholar. The following keyword combinations were employed in the search process: "Lung cancer," "Radiotherapy for lung cancer," "Lung segmentation," "Lung tumor segmentation," "Artificial intelligence." The queried results were imported into Endnote for deduplication [32], and there were 2183 literature items obtained after filtering. In this section, we used Endnote to analyze these papers.

Fig. (**2**) shows a chart of the relevant literature over the last 10 years. Fig. (**2a**) shows the publication trend: the number of articles published in this direction increased by 148% in the past three years, but the overall number of articles published remained low. Fig. (**2b**) is a keyword analysis diagram of papers in related areas in the past 10 years, among which DL accounts for a large proportion of the word cloud. To sum up, the data show that DSLC is a hot research topic that has emerged in recent years.

2.2. Literature Survey

Table **1** compares five review articles on OAR and LT segmentation and detection in the past five years. This survey mainly analyzed the deficiencies of the literature in terms of coverage, data indicators, and research trends.

The results in Table **1** indicate some limitations in the existing reviews. First, there is a lack of detailed reviews explaining the limitations of other studies and the motivation for their own research; second, there is a lack of analysis of research trends; third, there is a lack of evaluation of relevant research work, metric details, and dataset details; and fourth, there is a lack of discussion of current research challenges and possible solutions. We conducted a detailed DSLC survey in an attempt to fill the gaps in the existing literature.

2.3. Common Datasets for Lung Tumors

Some publicly available datasets are frequently used in the diagnosis and treatment of lung cancer using deep neural networks, as shown in (Table **2**).

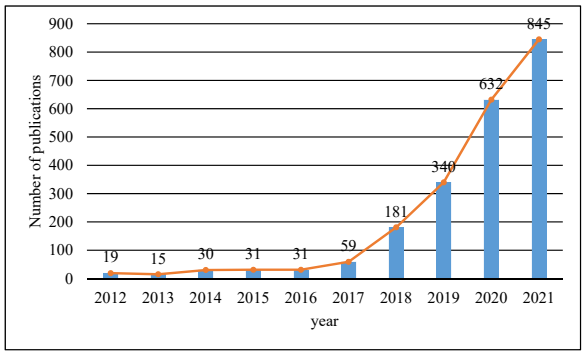

(**a**)

(**b**)

Fig. (2). Literature research and analysis in the past 10 years. (**a**) Post trend chart; the x-axis represents the input year and the y-axis represents the number of posts. (**b**) Keyword analysis chart. (*A higher resolution / colour version of this figure is available in the electronic copy of the article*).

Among the lung cancer datasets listed in Table **2**, the LIDC-IDRI dataset provides an authoritative and open standard for research on lung nodules [55, 56], and the details of other lung cancer-related datasets are also summarized in the table.

3. DEEP LEARNING AUTOMATIC SEGMENTATION TECHNOLOGY

3.1. Introduction to Deep Learning

DL has been widely used in image analysis in pathology [57-59]. The current popular DL algorithm includes a

Table 1. Detailed analysis of our study compared to existing reviews.

Refs.	Year	Literature Coverage Range	Type of Learning Methods	Main Theme	Existing Surveys are Reviewed	Analyzed Research Trend	Metrics Details	Datasets Details	Current Challenge, Solutions
[33]	2021	2013-2020	Deep Learning	Multi-organ segmentation	NO	YES	NO	NO	NO
[34]	2020	2017-2019	Traditional	Multi-organ tumor detection	NO	NO	NO	NO	NO
[35]	2019	2017-2019	Deep Learning	Lung cancer image analysis	NO	NO	NO	NO	NO
[36]	2018	2009-2018	Deep Learning and Traditional	Lung nodule detection	NO	NO	YES	NO	NO
[37]	2021	2017-2020	Deep Learning	Multi-organ segmentation and lung tumor segmentation	NO	NO	NO	NO	YES
[38]	2022	2013-2021	Deep Learning	Lung tumor segmentation	NO	NO	NO	NO	NO
OURS	2022	2018-2021	Deep Learning	Multi-organ segmentation and lung tumor segmentation	YES	YES	YES	YES	YES

Table 2. Public lung tumor datasets.

Dataset	Year	Input	Details	Refs.
Non-small cell lung cancer (NSCLC)	2021	CT/ PET-CT	285,411 images with a total data capacity of 97.6 GB	[39]
LIDC-IDRI	2020	CT/DX/CR	244,527 images with a total data capacity of 125 GB	[40]
Lung CT Segmentation Challenge 2017	2020	CT	9593 images with a total data capacity of 4.8 GB	[41]
NIH	2019	CT	32,735 images with a total data capacity of 221 GB	[42]
NLST	2017	CT	Over 75,000 CT images in 15 sub-databases	[43]
Data Science Bowl 2017	2017	CT	The National Cancer Institute's Center for Cancer Research provides a two-stage dataset; the data capacity of the first stage exceeds 66 GB, and that of the second stage exceeds 38 GB	[44]
ChestX-ray14	2017	X-Ray	112,120 images with a total data capacity of 45 GB	[45]
QIN LUNG CT	2017	CT	3954 images with a total data capacity of 2.08 GB	[46]
LUNA16	2016	CT	888 CT images of 1084 tumors	[47]
SPIE-AAPM Lung CT Challenge	2016	CT	22,489 images with a total data capacity of 12.1 GB	[48]
LungCT-Diagnosis	2014	CT	4682 images with a total data capacity of 2.5 GB	[49]
TCIA	2021	MRI/CT	Large-scale public database containing medical images such as common tumors and corresponding clinical information, with all data organized and managed by TCIA.	[50]
TCGA	2021	MRI/CT	11,961 lung cases with a total data capacity of 2.5 PB	[51]
CLEF 2017	2017	N/A	CLEF dataset includes 500 patients, categorized into five TB types: invasive, focal, tubercular, miliary, and cavernous fibroma.	[52]
SCR	2000	X-Ray	247 chest X-rays, including left and right lung, left and right clavicle, heart, *etc*. Total data capacity of 2.5 MB	[53]
JSRT	2000	CT/X-Ray	154 conventional CT chest radiographs, the total data capacity of 1.33 GB	[54]

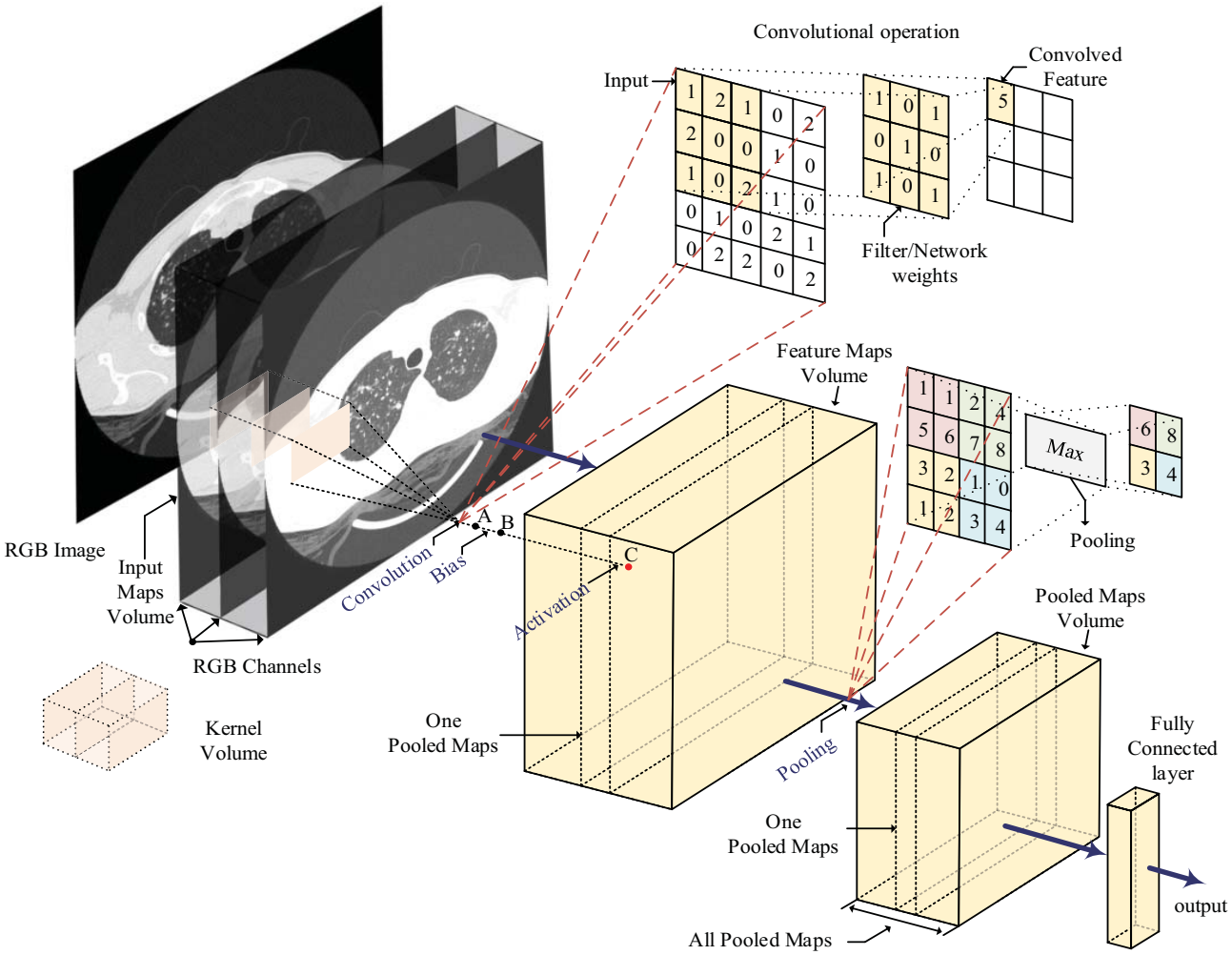

Fig. (3). Convolutional neural network (CNN) structure diagram. (*A higher resolution / colour version of this figure is available in the electronic copy of the article*).

convolutional neural network (CNN) [60] and generative adversarial network (GAN) [61]; the latter has the characteristics of unsupervised learning [62]. Some scholars integrate GAN and CNN for medical image segmentation. Based on the wider application of CNN, in this paper, we focus on the application of CNN in DSLC. CNN contains convolutional, pooling, and fully connected layers. The role of the convolutional layer is to use the convolution kernel to extract features from the input image. The role of the pooling layer is to reduce the resolution of the feature map and the consumption of memory. The role of the fully connected layer is to classify and output the extracted features. The structure diagram of CNN is shown in Fig. (**3**).

Commonly used basic CNNs are VGG [63] and ResNet [64]. VGG is a network model with a simple structure and strong generalization ability. VGG increases the receptive field by stacking small convolution kernels. ResNet is based on the concept of using shortcut connections to solve the problem of deep network degradation so that thousands of layers of convolutional networks can converge.

In addition to the basic convolutional network, there are two commonly used segmentation neural networks, FCN [65] and U-Net [66]. FCN uses a skip connection structure to fuse the shallow appearance information and deep semantic information of the feature map to segment images more accurately. U-Net has a better processing effect for medical image data with a small amount of data, large image size, blurred boundaries, and multi-modal imagery, and has become the baseline for most medical image semantic segmentation tasks. In addition, the derived Attention U-Net [67] further improves the performance of image segmentation.

3.2. Common Evaluation Indicators

Table **3** lists the metrics commonly used in experiments; among them, the dice similarity coefficient (DSC) is a simple and useful statistical validation metric that can be applied to study the accuracy of image segmentation [68].

3.3. LT and OAR Segmentation for Lung Cancer

Patients with advanced lung cancer have a five-year survival rate of less than 15%, but survival rates after treatment for early-stage lung cancer can range from 40 to 70% [75]. As a result, early detection and treatment are critical to in-

Table 3. Evaluation parameters.

Parameter	Description	Mathematical Equation	Refs.
TP	True positive; the number of positive examples correctly divided	N/A	[69]
FP	False positive; the number of false positives	N/A	[69]
FN	False negative; number falsely classified as negative	N/A	[69]
TN	True negative; number correctly divided into negative examples	N/A	[69]
PRE	Precision; the ratio of true positives among predicted positive samples	$\frac{TP}{TP+FP}$	[69]
DSC	Dice similarity coefficient; measures the degree of overlap between two segmentations, where R = segmenting contour and S = ground truth resulting from manual segmentation	$D(R,S)=\frac{2\lvert R\cap S\rvert}{\lvert R\rvert+\lvert S\rvert}$	[70]
JS	Jaccard similarity; used to compare similarity and diversity of image, where R = segmented image, S = ground truth, and higher value = better segmentation	$J(R,S)=\frac{\lvert R\cap S\rvert}{\lvert R\cup S\rvert}$	[71]
SP	Specificity; defines the proportion of identified counterexamples	$\frac{TN}{TN+FP}$	[72]
SN	Sensitivity; refers to the proportion of all positive examples identified	$\frac{TP}{TP+FN}$	[72]
ACC	Accuracy; the ratio of the number of correct classifications	$\frac{TP+TN}{TP+FP+TN+FN}$	[72]
HD95%	Hausdorff distance 95%; HD95% = 0.95 $\times d_H\{X,Y\}$, used to describe the similarity between two sets of points	$d_H\{X,Y\}=max\{d_{XY},d_{YX}\}$ $=max\begin{Bmatrix}max_{x\in X}min_{y\in Y}d\{x,y\},\\max_{y\in Y}min_{x\in X}d\{x,y\}\end{Bmatrix}$	[73]
MSD	Mean surface distance; an average of two directed average Hausdorff measures	$\frac{1}{2\lvert X\rvert}\sum_{x\in\lvert X\rvert}min_{y\in\lvert Y\rvert}d(x,y)$ $+\frac{1}{2\lvert Y\rvert}\sum_{y\in\lvert Y\rvert}min_{x\in\lvert X\rvert}d(y,x)$	[73]
VE	Volume error; $\lvert V_A\rvert$ denotes the foreground volume of the segmentation result and $\lvert V_R\rvert$ denotes volume of ground truth; volume difference is measured by VE	$VE(V_A,V_R)=\frac{abs(\lvert V_A\rvert-\lvert V_R\rvert)}{\lvert V_R\rvert}$	[74]
CE	Classification error; $\lvert V_{FP}\rvert$ denotes the total number of voxels with false positive error and $\lvert V_{FN}\rvert$ denotes the total number of voxels with false negative error; spatial location bias of segmented foreground is measured by CE	$CE(V_A,V_R)=\frac{\lvert V_{FP}\rvert+\lvert V_{FN}\rvert}{\lvert V_R\rvert}$	[74]

creasing the cure rate [76]. The primary treatment method for lung cancer is RT. In clinical practice, precise irradiation of tumor target areas and protection of OARs are critical factors for RT success, and DSLC plays an important role in these tasks. This section discusses and compares DSLC-related work from two perspectives: LT segmentation and OAR segmentation (Fig. **4**).

3.3.1. Lung Tumor Segmentation

In the diagnosis of clinical lung tumors (LTs), it is often necessary to process images of different modalities, such as X-ray, computed tomography (CT), ultrasound, magnetic resonance imaging (MRI), positron emission tomography (PET), and positron emission computed tomography (PET-CT), as shown in Fig. (**4**).

Zhang *et al*. [77] developed an improved ResNet for segmenting of non-small-cell lung tumors on CT images, combining shallow and deep semantic features to produce dense pixel output. In 2020, Pang *et al*. [78] proposed CTumorGAN, a unified end-to-end adversarial learning framework, for the prediction of CT images using multi-level supervision of different modules to deal with problems such as class imbalance, small tumors, and label noise, with a DSC coefficient of 71.08%. With a success rate of 99.92%, the method improves the model's generalization ability for different objective functions and achieves a stable tumor segmentation scheme with a low error rate. Jiang J. *et al*. [79] developed a cross-modal (MR-CT) depth learning segmentation method, which enhances training data by converting manually segmented CT images into pseudo-MR images.

MRI provides high resolution for soft tissue, allowing a better view of tumors and adjacent normal tissues. Wang *et al*. [29] presented A-Net, a new patient-specific adaptive convolutional neural network that uses MRI imags and GTV annotation to train the network model; its DSC index and precision are 0.82 0.10 and 0.81 0.08, respectively Jiang *et al*. [80] developed a cross-modality induced distillation method for cone-beam CT (CBCT) images. The idea is to use MRI to guide the training of the CBCT segmentation network.

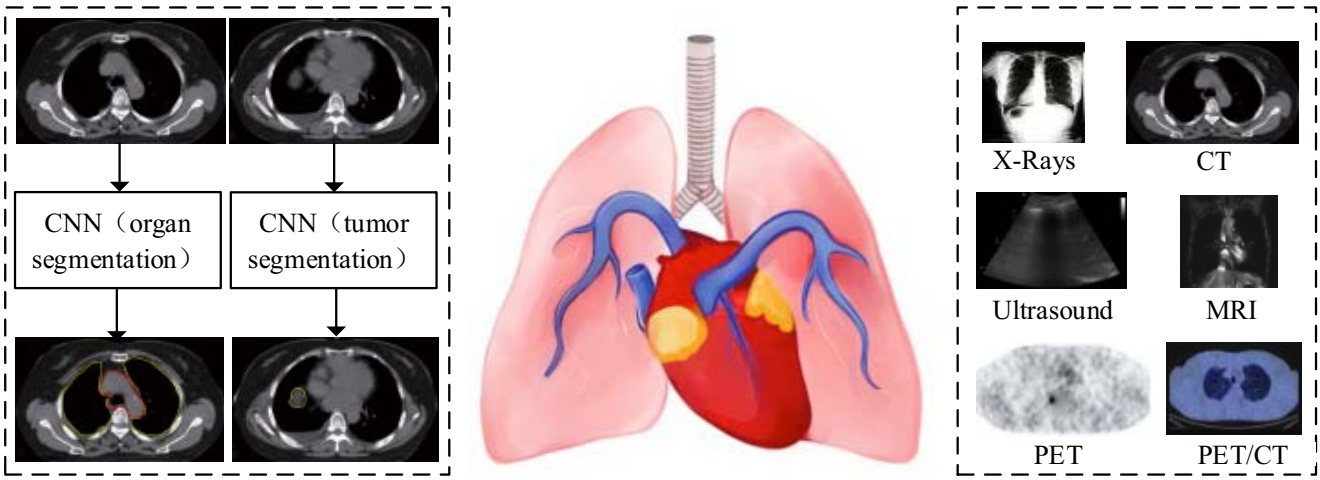

Fig. (4). Segmentation of lung tumors (LTs) and organs at risk (OARs) for lung cancer. (*A higher resolution / colour version of this figure is available in the electronic copy of the article*).

The advantage of PET is that it can accurately locate small tumors and distinguish benign and malignant tumors early. Leung *et al*. [81] proposed mU-Net for segmenting of PET images, which is designed to help address the challenge of a lack of clinical training data with known ground-truth tumor boundaries in PET.

PET-CT combines the high sensitivity of PET images with the anatomical information of CT images and overcomes the difficulties of blurred image boundaries, low contrast, and complex backgrounds. Zhao *et al*. [74] proposed a multimodal segmentation method based on 3D full convolution neural network, which can extract the characteristic information of PET and CT simultaneously for tumor segmentation, and has strong robustness. In 2020, Li *et al*. [82] integrated CT tumor probability maps and PET images into a recognition model, which could accurately identify the input images. In 2021, Lei *et al*. [83] proposed a recurrent fusion network (RFN) for automatic PET-CT tumor segmentation that can complementarily fuse the intermediate segmentation results to obtain multi-modal image features, which improves the convergence speed. Fu *et al*. [84] proposed a multi-modal spatial attention network module (MSAM).

In addition, Bi *et al*. [85] established a deep expansion residual network based on ResNet-101, which is used to automatically sketch the CTV of lung cancer patients undergoing radiotherapy after surgery. The experimental results show that, compared with manual contour, the effect of deep learning assisted sketching is better, and 35% of the time is saved than before. Jemaa *et al*. [86] proposed an end-to-end method to quickly identify and segment tumors by combining 2D and 3D convolutional networks, which can adapt to an extreme imbalance between healthy tissue volumes and heterogeneity of input images. Jiang *et al*. [87] developed two multiresolution residual connection networks, combined the features and functional levels of multiple image resolutions, and detected and segmented lung tumors through residual connection. After evaluation, it can accurately segment the volume of lung tumors.

Table **4** lists the lung tumor segmentation work in detail. Fig. (**5**) shows the DSC accuracy of lung tumor segmentation in the related literature, where the abscissa represents the reference numbers in Table **4** and the ordinate represents the DSC values, which are mostly above 0.7 [88].

3.3.2. Organ-at-Risk Segmentation

Because RT can affect organs outside the target area, radiation oncologists must accurately segment OARs to reduce the probability of normal tissue complications after RT. DL segmentation models can now automatically segment OARs based on trial and error. This section discusses various methods for solving the difficult problem of automatic OAR segmentation, such as experimenting with different network architectures, introducing loss functions, and combining supervised and unsupervised learning methods, which will be discussed in detail below. Zhu *et al*. [89] improved the deep learning split network based on U-Net, which can split many kinds of OARs in the lung. Among them, the DSC index for segmenting the lung is the highest, reaching 95%. Feng *et al*. [73] proposed a based 3D U-Net model to automatically segment five sternal OARs, including the left and right lungs, heart, esophagus, and spinal cord. Based on U-Net, Vesal *et al*. [90] used the expansion convolution and aggregation residual connection methods to segment OARs in chest CT images, and achieved high-precision segmentation of 20 undiscovered test samples.

GAN [61] can produce quite good output through mutual game learning of generative and discriminative models. Dong *et al*. [91] proposed a UNet-GAN strategy to automatically delineate the left and right lungs, spinal cord, esophagus, and heart. With the assistance of adversarial networks, the segmentation accuracy was greatly improved. It has been found in experiments that the traditional convolutional neural network model is not very compatible with medical imaging. He *et al*. [92] proposed a unified encoder–decoder architecture based on the U-Net model and used it in multi-task procedures. It is trained in learning mode, and the experimental results show that the DSC accuracy on the heart reaches 95%.

Table 4. Selected works on deep learning-based automated segmentation of lung tumors (LTs).

Team	DataSets	Input	Net	Evaluation Metrics	Research Highlights
Wang *et al*. (2018) [29]	9 patients	MRI	ANet	**DSC** 0.82 ± 0.10 **PRE** 0.82± 0.08 **SN** 0.85 ± 0.13	Adaptive neural network, A-Net, was introduced to delineate LTs
Zhao *et al*. (2018) [74]	84 patients	PET-CT	3D FCN	**DSC** 0.85 ± 0.08	Novel multimodal segmentation network, 3D FCN, proposed to integrate PET and CT images into the same utility
Jiang *et al*. (2018) [87]	1210 patients TCIA MSKCC LIDC	CT	MRRN	**DSC** **HD95%** **SN** **PRE** **TCIA** 0.74 7.94 0.80 0.73 **MSKC** 0.75 5.85 0.82 0.72 **LIDC** 0.68 2.60 0.85 0.67	Multi-resolution residual connection network proposed to combine features across multiple image resolution through residual connections to detect and segment LTs
Bi *et al*. (2019) [85]	269 patients	CT	ResNet	**DSC** 0.75 ± 0.06 **CV** 0.129±0.04 **SDD** 0.47±0.22	ResNet network used to segment LTs, obtaining better results than manual segmentation
Jiang J.*et al*. (2019) [79]	28 patients	MR -CT	U-Net + cross modality	**DSC** 0.75 ±0.12 **VR** 0.19±0.15 **HD95%** 9.36±6.00	Cross-modal deep learning (DL) segmentation method used to better segment LTs
Li *et al*. (2020) [82]	84 patients	PET-CT	3D FCN	**DSC** 0.86 ± 0.05 **VE** 0.16±0.12 **CE** 0.30±0.12	CT tumor probability maps and PET intensity images combined for accurate multimodal tumor segmentation
Zhang *et al*. (2020) [77]	330 patients	CT	ResNet	**DSC** 0.73±0.07 **JS** 0.68±0.09 **SN** 0.74±0.07	Fast segmentation of LTs using improved ResNet
Pang *et al*. (2020) [78]	NSCLC	CT	CTumor-GAN	**DSC** 0.7108 **PRE** 0.7734 **SN** 0.7042	Authors propose CTumorGAN algorithm for better segmentation of LTs
Leung *et al*. (2020) [81]	30 patients	PET	mU-Net	**DSC** 0.73 **JS** 0.65 ±0.02 **HD95%** 3.25±0.30	mU-N*et al*gorithm was used to segment smaller LTs on slices of PET
Jemaa *et al*. (2020) [86]	3664 trial scans	PET-CT	2D and 3D architecture	**Lymphoma** **Lung** **SN** 0.926 0.93 **DSC** 0.886 N/A	Combined with 2D and 3D convolutional networks, rapid detection and segmentation of LTs were realized
Fu *et al*. (2021) [84]	876 NSCLC 3063 soft tissue sarcoma (STS) [88]	PET-CT	MSAM	**NSCLC** **STS** **DSC** 0.7144 0.6226 **PRE** 0.7293 0.69 **SN** 0.8109 0.6494 **SP** 0.9995 0.9974	Based on attention mechanism, a multimodal spatial attention network module (MSAM) is proposed to strengthen learning of tumor-related
Lei *et al*. (2021) [83]	70 patients	PET-CT	RFN	**DSC** 0.6775±0.2341 **PRE** 0.7164±0.2728 **SN** 0.7318±0.2558	RFN network is proposed to segment LTs

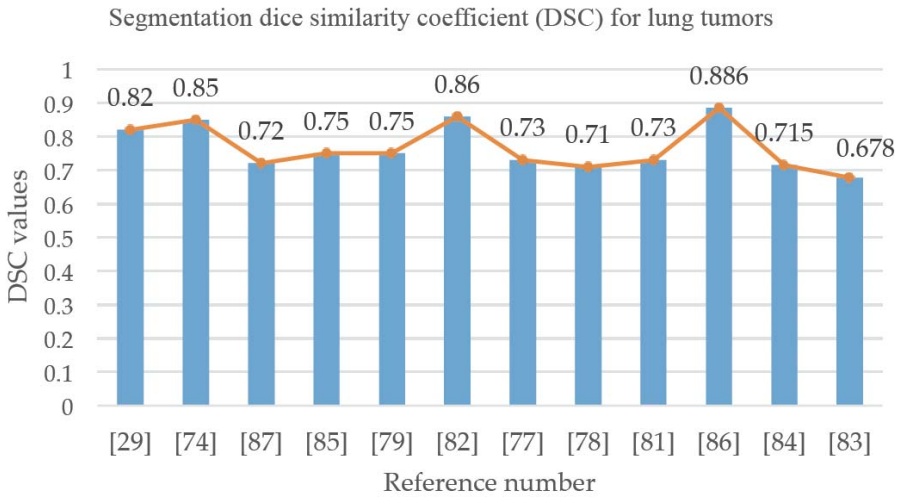

Fig. (5). Segmentation dice similarity coefficient (DSC) for lung tumors. (*A higher resolution / colour version of this figure is available in the electronic copy of the article*).

Zhao *et al*. [64] introduced multi-instance loss and conditional adversarial loss based on the FCN network to solve the segmentation problem under more severe pathological conditions, and the experiment obtained a DSC of 97.93%. Chen *et al*. [93] designed a weighted DSC based on the loss function of the coefficients is used to solve the problem of segmentation imbalance, and the experiment obtained a DSC of 97.55%.

The biggest challenge of DL in the medical field is the lack of annotated training sets. Hu *et al*. [94] used the Mask R-CNN architecture to combine supervised and unsupervised machine learning methods to automatically segment lungs on CT images and obtained the best results for lung segmentation. Research on automatic segmentation of OARs is not only important for radiotherapy but also provides inspiration and implications for other image segmentation algorithms.

Harten *et al*. [95] proposed various segmentation technologies based on different frameworks in combination with 2D-CNN and 3D-CNN to automatically segment four OARs: heart, aorta, trachea, and esophagus. The experimental results show that the best performance is achieved in DSC and HD. Akila *et al*. [96] proposed a convolutional deep wide network (CDWN) to segment lung regions in thoracic CT images. In the experiment, the DSC and ACC of the LIDC-IDRI dataset reached 95% and 98% respectively. Zhang, *et al*. [97] established a CNN network based on ResNet-101 for automatic segmentation of OARs, including lungs, esophagus, heart, liver, and spinal cord.

Table **5** details related work on OAR segmentation. Fig. (**6**) depicts the DSC accuracy for OAR segmentation in the searched literature, where the abscissa represents the reference numbers in Table **5** and the ordinate represents the DSC values, which are mostly above 0.8.

4. DISCUSSION

Although recent studies show that DSLC outperforms traditional segmentation methods in terms of efficiency and accuracy [100], it still faces some challenges.

4.1. Medical Imaging Problems

Tissues and organs in medical images have a high degree of similarity, especially in low-contrast images, where the segmentation target is very similar to the background and it is difficult to distinguish the boundaries. In terms of medicine, MRI images are preferable to CT as input because they provide better visualization [101]. In computer technology, new algorithms can be developed for solving the low-contrast problem of medical image segmentation. For example, 3D algorithmic networks should be used because they can adequately extract contextual spatial information from medical images compared to 2D networks, alleviating the problem of low contrast [102].

4.2. Dataset Size Issue

Obtaining medical images involves patient privacy issues, and the production of medical datasets requires professional doctors to label them. These two reasons lead to a scarcity of large medical datasets. However, training the model without a large number of samples hurts the robustness of the DL algorithm, resulting in overfitting of the trained model, and the small dataset cannot demonstrate the algorithm's generalization ability. These issues make the clinical application of DSLC more difficult. Moreover, apart from the datasets provided by some competitions with common standards, the datasets used by most researchers are of uneven quality, and the datasets created using specific scenarios to verify the overall performance of the algorithms are not convincing. In particular, most DSLC studies are based on single-point dataset training, which lacks diversity, and medical images in real situations have great differences due to race, age, gender, disease, *etc*., resulting in decreased model segmentation accuracy.

In light of the scarcity of medical datasets, various medical institutions could build large-scale datasets by sharing data in order to provide DL researchers with more expert annotated data under the premise of protecting patient privacy [103]. From the perspective of computer technology, DL researchers can also try to use transfer learning strategies

Table 5. Selected works on deep learning-based automated segmentation of OARs for lung cancer.

Team	DataSets	In	OARs	Network	DSC Metric	Other Evaluations Metric	Research Highlights
Zhao *et al.* (2018) [64]	LIDC-IDRI CLEF HUG [98]	CT	Lung	FCN	**LIDC**:0.9176 **CLEF**:0.9613 HUG**:0.9793**	**N/A**	Introduced multi-instance loss and conditional adversarial loss functions
Zhu *et al.* (2019) [89]	66 case of CT (30 case train, 36 case test)	CT	Lung Heart Esophagus Spinal cord liver	AdaptedU-Net	**Lung:**0.95±0.01 **Esophagus:**0.71±0.05 **Spinal cord:**0.79±0.03 **Heart:**0.91±0.03 Liver:**0.89±0.02**	**Lung:** 1.93±0.51(**MSD**) 7.96±2.57(**HD 95%**) **Esophagus:** 2.18±0.80(**MSD**) 7.83±2.85(**HD 95%**) **Spinal cord:** 1.25±0.23(**MSD**) 4.01±2.05(**HD 95%**) **Heart:** 2.92±1.51(**MSD**) 7.98±4.56(**HD 95%**) Liver:**3.21±0.93(** MSD**)**	Encoder–decoder U-Net neural network constructed based on convolutional neural networks (CNN) to automatically segment OARs
Harten *et al.* (2019) [95]	Seg Thor (60 thoracic CT scans)	CT	Heart Aorta Trachea esophagus	CNN	**Esophagus:**0.84±0.05 **Heart:**0.94±0.02 **Aorta:**0.93±0.01 Trachea:**0.91±0.02**	**HD** **Esophagus** 3.4±2.3 **Heart** 2.0±1.1 **Aorta** 2.7±3.6 Trachea **2.1±1.0**	2DCNN and 3DCNN frameworks combined to segment multiple organs at risk on chest CT
Akila *et al.* (2020) [96]	LIDC-IDRI	CT	Lung	CDWN	**0.95 ± 0.03**	**JS**:0.91 ± 0.04 **ACC**0.98 ± 0.01 **SP:**0.99±0.01 SN:**0.95 ±0.03** PRE:**0.95±0.03**	CDWN proposed for segmentation of lung regions in chest CT images
Dong *et al.* (2019) [91]	35 patiens	CT	Left lung Right lung Heart Esophagus Spinal cord	Unet-GAN	**Left Lung**0.97±0.01 **Right Lung**0.97±0.01 **Esophagus**0.75±0.08 **Spinal cord**0.90±0.04 Heart**0.87±0.05**	**Left Lung:** 0.61±0.73(**MSD**) 0.9989±0.0010(**SP**) 0.97±0.02**(SN)** 2.07±1.93(**HD 95%**) **Right Lung:** 0.65±0.53(**MSD**) 0.9992±0.0007(**SP**) 0.96±0.02(**SN**) 2.50±3.34(**HD 95%**) **Esophagus:** 1.05±0.66(**MSD**) 4.52±3.81(**HD 95%**) **Spinal cord:** 0.38±0.27(**MSD**) 1.19±0.46(**HD 95%**) **Heart:** **1.49±0.85(** MSD**) 4.58±3.67(**HD 95%)	U-Net used as generator and FCN as discriminator to design U-Net generative adversarial network (U-Net-GAN) to segment OARs in lung CT images
Feng *et al.* (2019) [73]	60 thoracic CT scans	CT	Left lung Right lung Heart Esophagus Spinal cord	3D U-Net	**Left Lung**0.98±0.01 **Right Lung**0.97±0.02 **Esophagus**0.73±0.09 **Spinal cord**0.89±0.04 Heart**0.93±0.02**	**Left Lung:** 0.59±0.29(**MSD**) 2.10±0.94(**HD 95%**) **Right Lung:** 0.93±0.57(**MSD**) 3.96±2.85(**HD 95%**) **Esophagus:** 2.34±2.38(**MSD**) 8.71±10.59(**HD 95%**) **Spinal cord:** 0.66±0.25(**MSD**) 1.89±0.63(**HD 95%**) **Heart :** **2.30±0.49(**MSD**) 6.57±1.50(**HD 95%)	Novel DCNN method proposed for automatic segmentation of chest OARs from large 3D images
Hu *et al.* (2020) [94]	1265 images	CT	Lung	Mask R-CNN	0.9733 ± 0.0324	**SN:**0.97 ± 0.09 **SP:**0.9711 ± 0.0365	Improved lung segmentation performance using a combination of Mask R-CNN and K-means

(Table 5) contd….

Team	DataSets	In	OARs	Network	DSC Metric	Other Evaluations Metric	Research Highlights
Vesal *et al.* (2019) [90]	60 patients	CT	Heart Aorta Trachea esophagus	2D Unet	**Esophagus:**0.858 **Heart** 0.941 **Aorta** 0.938 **Trachea**0.926	**HD** **Esophagus** 0.331 **Heart** 0.226 **Aorta** 0.297 **Trachea** 0.193	Introduced extended convolution in two-dimensional U-Net to better segment OARs
He *et al.* (2019) [92]	SegTHOR [99]	CT	Heart Aorta Trachea esophagus	Unet	**Esophagus:**0.8594 **Heart :**0.9500 **Aorta:** 0.9484 **Trachea:**0.9201	**HD** **Esophagus** 0.2743 **Heart** 0.1383 **Aorta** 0.1129 **Trachea** 0.1824	Optimized false positive filtering algorithm to decrease number of falsely segmented organ pixels
Zhang *et al.* (2020) [97]	250 patients	CT	Left lung Right lung Heart Esophagus Spinal cord liver	AS-CNN	**Left lung**0.948±0.013 **Left lung**0.943±0.015 **Esophagus**0.732±0.069 **Spinal cord**0.821±0.046 **Heart**0.893±0.048 **liver**0.937±0.027	**MSD**: **Left Lung**1.10±0.15 **Right Lung**2.23±2.33 **Esophagus**1.38±0.44 **Spinal cord**0.87±0.21 **Heart** 1.65±0.48 **Liver** 2.03±1.49	AS-CNN algorithm proposed, proving that DL is better than atlas method in automatic organ segmentation
Chen *et al.* (2019) [93]	45 thorax DECT	DECT	Left lung Right lung Liver Spleen Left Kidney Right Kidney	3D FCN	**L_lung**0.975±0.0064 **R_lung**0.976±0.0161 **Liver**0.962±0.0164 **Spleen:**0.914±0.0486 **L_Kidney:**0.937±0.0312 **R_Kidney:**0.945±0.0122	**HD** **Left Lung:** 6.97±2.67 **Right Lung:** 8.08±3.51 **Liver:** 9.64±4.89 **Spleen:**6.93±3.44 **Left Kidney**:4.41±2.17 **Right Kidney:**3.62±1.75	Multiple 3D CNNs proposed for segmentation of multi-organ DECT images

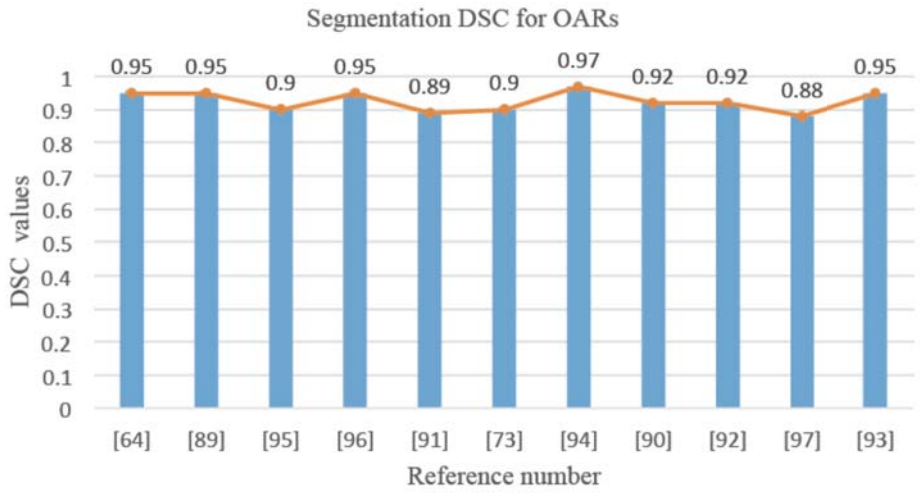

Fig. (6). Segmentation DSC for OARs. (*A higher resolution / colour version of this figure is available in the electronic copy of the article*).

[104] to pre-train network models as a way to alleviate the problem of limited data. Furthermore, medical image datasets can also be augmented by cropping, rotating, filling, and color-enhancing images through data augmentation methods.

4.3. Algorithmic Model Problems

The deeper the layers of the network model, the stronger the ability to extract features and the more complex the network structure. For the pixel-by-pixel classification task of lung images, expanding the number of layers of the network model is conducive to training a more accurate segmentation model. In addition, in order to extract and fuse multi-scale features of images, most researchers try to use more strategies for extracting features in the network, which undoubtedly increases the complexity of the network structure. As the number of network layers of the model increases, the ability

to extract features, the data occupied by the GPU memory, and the time to train the model increase at the same time. Most algorithms reduce the training time by sacrificing a large amount of GPU space. This is not a long-term solution, and complex network structure has become a technical barrier limiting the improvement of model segmentation accuracy. It is worth considering how to strike a balance between network design, computing time, and cost. Hu *et al*. [94] used the improved Mask R-CNN architecture to achieve high-precision segmentation in DSC and combined it with the K-means method to improve the segmentation accuracy while reducing the model structure. At the same time, to avoid the constraints of GPU memory, we can try to use algorithms such as GAN to generate training data artificially to reduce the number of hidden layers or parameters of the network and to overcome hardware constraints to a certain extent.

4.4. Clinical Application Issues

The biggest difference between clinical medical applications and the experimental process is that there will be various unpredictable clinical situations [105]. If the DSLC only operates in a data environment similar to the training dataset, it will be difficult to respond correctly to emergencies. DSLC is required to be able to continuously learn to cope with clinical emergencies. In addition, DL algorithms also lack interpretability, it is difficult to fully understand which factors in the algorithm will lead to degraded segmentation performance, and it may not be possible to control the stability of OAR segmentation and GTV accuracy. If this uncertainty is used in clinical practice, it is very dangerous. Before DSLC is used clinically, relevant hospital personnel should conduct a thorough risk assessment, consider legal and ethical responsibilities, think about measures to deal with emergencies, and formulate a set of detailed standard procedures to protect the safety of patients. Computer-related researchers can also explore new network frameworks that enable models to learn experiences autonomously under unknown conditions, improve models' continuous learning ability, and reduce clinical application risks.

CONCLUSION

In this paper, we investigated many kinds of studies, extracted common datasets and evaluation indicators for LTs, reviewed the basic theory of DL-related algorithms, and discussed and compared DSLC-related work from two aspects of LT and OAR segmentation. By improving the network framework and the segmentation accuracy, DSLC achieved satisfactory results in OAR segmentation of the lung and heart. However, it also has some challenges. To address these challenges, this paper presents an analysis and possible solutions. The author's knowledge is limited, and some important works may not be included in this paper. Hopefully, this review will deepen researchers' understanding of lung cancer RT and DL, and stimulate collaboration between the two communities to develop a more specialized adjuvant lung cancer RT application system.

LIST OF ABBREVIATIONS

ACC	=	Accuracy
CBCT	=	Cone-beam CT
CE	=	Classification Error
CNN	=	Convolutional Neural Networks
CT	=	Computed Tomography
CTV	=	Clinical Target Volume
DL	=	Deep Learning
DSC	=	Dice Similarity Coefficient
DSLC	=	Deep Learning-Based Segmentation Technology for Lung Cancer Radiotherapy
GAN	=	Generative Adversarial Network
GTV	=	Gross Tumor Volume
HD95%	=	Hausdorff_Distance95%
JS	=	Jaccard Similarity
LTs	=	Lung Tumors
MRI	=	Magnetic Resonance Imaging
MSAM	=	Multi-Modal Spatial Attention Network Module
MSD	=	The Mean Surface Distance
NSCLC	=	Non-Small Cell Lung Cancer
OARs	=	Organs at Risk
PET	=	Positron Emission Tomography

CONSENT FOR PUBLICATION

Not applicable.

FUNDING

This work was financially supported by the Natural Science Foundation of Anhui Provincial (Grant No. 1808085MF202), the Talent project of Anhui Provincial (Grant No. gxgwfx200050), the Natural Science Research Project of Anhui Provincial (Grant No. KJ2021A0662), the Science Research and Innovation Team of Fuyang Normal University (Grant No. kytd202004), the Natural Science Research Project of Fuyang Normal University (Grant No. 2018kyqd0028, 2021FSKJ02ZD). My project name is An-Hui Provincial Graduate Innovation and Entrepreneurship Practice Project, and Grant No. 2022cxcysj189.

CONFLICT OF INTEREST

The authors have no conflicts of interest, financial or otherwise.

ACKNOWLEDGEMENTS

Y.W. conceptualized and presented the idea; J.H., T.L. studied the state-of-the-art methods and summarized the literature and prepared the draft; All authors provided feedback, helped shape the research, and contributed to the final manuscript. All authors have read and agreed to the published version of the manuscript.

REFERENCES

[1] Bray F, Laversanne M, Weiderpass E, Soerjomataram I. The ever-increasing importance of cancer as a leading cause of premature death worldwide. Cancer 2021; 127(16): 3029-30. http://dx.doi.org/10.1002/cncr.33587 PMID: 34086348

[2] Sung H, Ferlay J, Siegel RL, *et al.* Global cancer statistics 2020: GLOBOCAN estimates of incidence and mortality worldwide for 36 cancers in 185 countries. CA Cancer J Clin 2021; 71(3): 209-49. http://dx.doi.org/10.3322/caac.21660 PMID: 33538338

[3] Latest global cancer data: Cancer burden rises to 19.3 million new cases and 10.0 million cancer deaths in 2020. 2020. Available from: https://web.archive.org/web/202 20301120144/https://www.iarc.who.int/wp-content/upl oads/2020/12/pr292_E.pdf (Accessed on: 12 february 2022).

[4] Vinod SK, Hau E. Radiotherapy treatment for lung cancer: Current status and future directions. Respirology 2020; 25(Suppl. 2): 61-71. http://dx.doi.org/10.1111/resp.13870 PMID: 32516852

[5] Nagata Y, Kimura T. Stereotactic body radiotherapy (SBRT) for Stage I lung cancer. Jpn J Clin Oncol 2018; 48(5): 405-9. http://dx.doi.org/10.1093/jjco/hyy034 PMID: 29635536

[6] Brown S, Banfill K, Aznar MC, Whitehurst P, Faivre Finn C. The evolving role of radiotherapy in non-small cell lung cancer. Br J Radiol 2019; 92(1104): 20190524. http://dx.doi.org/10.1259/bjr.20190524 PMID: 31535580

[7] Burdett S, Rydzewska L, Tierney J, *et al.* Postoperative radiotherapy for non-small cell lung cancer. Cochrane Database System Rev 2016; 10(10): CD002142. http://dx.doi.org/10.1002/14651858.CD002142.pub3

[8] Baker S, Dahele M, Lagerwaard FJ, Senan S. A critical review of recent developments in radiotherapy for non-small cell lung cancer. Radiat Oncol 2016; 11(1): 115. http://dx.doi.org/10.1186/s13014-016-0693-8 PMID: 27600665

[9] Meyer P, Noblet V, Mazzara C, Lallement A. Survey on deep learning for radiotherapy. Comput Biol Med 2018; 98: 126-46. http://dx.doi.org/10.1016/j.compbiomed.2018.05.018 PMID: 29787940

[10] Samarasinghe G, Jameson M, Vinod S, *et al.* Deep learning for segmentation in radiation therapy planning: a review. J Med Imaging Radiat Oncol 2021; 65(5): 578-95. http://dx.doi.org/10.1111/1754-9485.13286 PMID: 34313006

[11] Daisne JF, Blumhofer A. Atlas-based automatic segmentation of head and neck organs at risk and nodal target volumes: a clinical validation. Radiat Oncol 2013; 8(1): 154. http://dx.doi.org/10.1186/1748-717X-8-154 PMID: 23803232

[12] Cabezas M, Oliver A, Lladó X, Freixenet J, Bach Cuadra M. A review of atlas-based segmentation for magnetic resonance brain images. Comput Methods Programs Biomed 2011; 104(3): e158-77. http://dx.doi.org/10.1016/j.cmpb.2011.07.015 PMID: 21871688

[13] Bai W, Shi W, Ledig C, Rueckert D. Multi-atlas segmentation with augmented features for cardiac MR images. Med Image Anal 2015; 19(1): 98-109. http://dx.doi.org/10.1016/j.media.2014.09.005 PMID: 25299433

[14] Meiburger KM, Acharya UR, Molinari F. Automated localization and segmentation techniques for B-mode ultrasound images: A review. Comput Biol Med 2018; 92: 210-35. http://dx.doi.org/10.1016/j.compbiomed.2017.11.018 PMID: 29247890

[15] Wang Y, Zhao L, Wang M, Song Z. Organ at risk segmentation in head and neck ct images using a two-stage segmentation framework based on 3D U-Net. IEEE Access 2019; 7: 144591-602.

[16] Liu C, Gardner SJ, Wen N, *et al.* Automatic segmentation of the prostate on CT images using deep neural networks (DNN). Int J Radiat Oncol Biol Phys 2019; 104(4): 924-32.

[17] Men K, Zhang T, Chen X, *et al.* Fully automatic and robust segmentation of the clinical target volume for radiotherapy of breast cancer using big data and deep learning. Phys Med 2018; 50: 13-9. http://dx.doi.org/10.1016/j.ejmp.2018.05.006 PMID: 29891089

[18] Avanzo M, Stancanello J, Pirrone G, Sartor G. Radiomics and deep learning in lung cancer. Strahlenther Onkol 2020; 196(10): 879-87. http://dx.doi.org/10.1007/s00066-020-01625-9 PMID: 32367456

[19] Liu Z, Yao C, Yu H, Wu T. Deep reinforcement learning with its application for lung cancer detection in medical Internet of Things. Future Gener Comput Syst 2019; 97: 1-9. http://dx.doi.org/10.1016/j.future.2019.02.068

[20] Polat H, Danaei Mehr H. Classification of pulmonary CT images by using hybrid 3D-deep convolutional neural network architecture. Appl Sci (Basel) 2019; 9(5): 940. http://dx.doi.org/10.3390/app9050940

[21] Vrtovec T, Močnik D, Strojan P, Pernuš F, Ibragimov B. Auto-segmentation of organs at risk for head and neck radiotherapy planning: From atlas-based to deep learning methods. Med Phys 2020; 47(9): e929-50. http://dx.doi.org/10.1002/mp.14320 PMID: 32510603

[22] Kholiavchenko M, Sirazitdinov I, Kubrak K, *et al.* Contour-aware multi-label chest X-ray organ segmentation. Int J CARS 2020; 15(3): 425-36. http://dx.doi.org/10.1007/s11548-019-02115-9 PMID: 32034633

[23] Tamang LD, Kim BW. Deep learning approaches to colorectal cancer diagnosis: A review. Appl Sci (Basel) 2021; 11(22): 10982. http://dx.doi.org/10.3390/app112210982

[24] Cao H, Liu H, Song E, *et al.* A two-stage convolutional neural networks for lung nodule detection. IEEE J Biomed Health Inform 2020; 24(7): 1. http://dx.doi.org/10.1109/JBHI.2019.2963720 PMID: 31905154

[25] Wong J, Fong A, McVicar N, *et al.* Comparing deep learning-based auto-segmentation of organs at risk and clinical target volumes to expert inter-observer variability in radiotherapy planning. Radiother Oncol 2020; 144: 152-8. http://dx.doi.org/10.1016/j.radonc.2019.10.019 PMID: 31812930

[26] Men K, Dai J, Li Y. Automatic segmentation of the clinical target volume and organs at risk in the planning CT for rectal cancer using deep dilated convolutional neural networks. Med Phys 2017; 44(12): 6377-89. http://dx.doi.org/10.1002/mp.12602 PMID: 28963779

[27] Souza JC, Bandeira Diniz JO, Ferreira JL, França da Silva GL, Corrêa Silva A, de Paiva AC. An automatic method for lung segmentation and reconstruction in chest X-ray using deep neural networks. Comput Methods Programs Biomed 2019; 177: 285-96. http://dx.doi.org/10.1016/j.cmpb.2019.06.005 PMID: 31319957

[28] Shaziya H, Shyamala K, Zaheer R. Automatic lung segmentation on thoracic CT scans using U-net convolutional network. 2018 International conference on communication and signal processing (ICCSP). 3-5 April 2018; Chennai, India: IEEE; pp 0643-7 http://dx.doi.org/10.1109/ICCSP.2018.8524484

[29] Wang C, Tyagi N, Rimner A, *et al.* Segmenting lung tumors on longitudinal imaging studies *via* a patient-specific adaptive convolutional neural network. Radiother Oncol 2019; 131: 101-7. http://dx.doi.org/10.1016/j.radonc.2018.10.037 PMID: 30773175

[30] Han M, Yao G, Zhang W, *et al.* Segmentation of CT thoracic organs by multi-resolution VB-nets. >SegTHOR@ ISBI; 8-11 April 2019; Venice, Italy

[31] Park J, Yun J, Kim N, *et al.* Fully automated lung lobe segmentation in volumetric chest CT with 3D U-Net: validation with intra- and extra-datasets. J Digit Imaging 2020; 33(1): 221-30. http://dx.doi.org/10.1007/s10278-019-00223-1 PMID: 31152273

[32] Hupe M. EndNote X9. J Electron Resour Med Libr 2019; 16(3-4): 117-9. http://dx.doi.org/10.1080/15424065.2019.1691963

[33] Fu Y, Lei Y, Wang T, Curran WJ, Liu T, Yang X. A review of deep learning based methods for medical image multi-organ segmentation. Phys Med 2021; 85: 107-22. http://dx.doi.org/10.1016/j.ejmp.2021.05.003 PMID: 33992856

[34] Sharif MI, Li JP, Naz J, Rashid I. A comprehensive review on multi-organs tumor detection based on machine learning. Pattern Recognit Lett 2020; 131: 30-7. http://dx.doi.org/10.1016/j.patrec.2019.12.006

[35] Wang S, Yang DM, Rong R, *et al.* Artificial intelligence in lung cancer pathology image analysis. Cancers (Basel) 2019; 11(11): 1673. http://dx.doi.org/10.3390/cancers11111673 PMID: 31661863

[36] Zhang G, Jiang S, Yang Z, *et al.* Automatic nodule detection for lung cancer in CT images: A review. Comput Biol Med 2018; 103: 287-300. http://dx.doi.org/10.1016/j.compbiomed.2018.10.033 PMID: 30415174

[37] Liu X, Li KW, Yang R, Geng LS. Review of deep learning based automatic segmentation for lung cancer radiotherapy. Front Oncol 2021; 2021: 11717039.

http://dx.doi.org/10.3389/fonc.2021.717039 PMID: 34336704
[38] Kao YS, Yang J. Deep learning-based auto-segmentation of lung tumor PET/CT scans: a systematic review. Clin Transl Imaging 2022; 10(2): 217-23. http://dx.doi.org/10.1007/s40336-022-00482-z
[39] Smith K, Nolan T. NSCLC Radiogenomics. Available from: https://web.archive.org/web/20220301 091241/https://wiki.cancerimagingarchive.net/display/Public/NSCLC+Radiogenomics (Accessed on: 11 February 2022).
[40] Vendt B, Nolan T. The Lung Image Database Consortium image collection. Available from: https: //wiki.cancerimagingarchive.net/display/Public/LIDC-IDRI (Accessed on: 3 January 2022).
[41] Nolan T, Jarosz Q. Lung CT segmentation challenge. 2017. Available from: ive.org/web/20220301131137/https://wiki.cancerimagingarchive.net/display/Public/Lung+CT+Segmentation+Challenge+2017 (Accessed on: 18 February 2022).
[42] DeepLesion. Available from: ive.org/web/20220301131812/https://nihcc.app.box.com/v/DeepLesion (Accessed on: 9 February 2022).
[43] NLST Datasets. Available from: rchive.org/web/20220301140337/https://cdas.cancer.gov/datasets/nlst/ (Accessed on: 5 February 2022).
[44] Data Science Bowl. 2017. Available from: https://www.kaggle.com/c/data-science-bowl-2017/ (Accessed on: 30 December 2021).
[45] NIH Chest X-rays. 2022. Available from: https:// www.kaggle.com/nih-chest-xrays/data/ (Accessed on: 12 February 2022).
[46] Smith K, Nolan T. QIN Lung CT. Available from: https://wiki.cancerimagingarchive.net/display /Public/QIN+LUNG+CT/ (Accessed on: 15 february 2022).
[47] Lung Nodule Analysis. 2016. Available from: https://web.archive.org/web/20220301142254/https://luna16.grand-challenge.org/Data/ (Accessed on: 8 February 2022).
[48] Kirby J, Jarosz Q. SPIE-AAPM Lung CT Challenge. Available from: https://web.archive.org/web/20220301142410/https://wiki.cancerimagingarchive.net/display /Public/SPIE-AAPM+Lung+CT+Challenge (Accessed on: 12 January 2022).
[49] Clark K, Jarosz Q. LungCT-Diagnosis. Available from: https://web.archive.org/web/202 2030 1143334/https://wiki.cancerimagingarchive.net/display/Public/LungCT-Diagnosis (Accessed on: 13 February 2022).
[50] Web Archive. The cancer imaging archive Available from: https://web.archive.org/web/20220302020242/https://www.cancerimagingarchive.net/ (Accessed on: 13 February 2022).
[51] TCGA. The Cancer Genome Atlas Program. Available from: https://web.archive.org/web/2022 0301143553/https://www.cancer.gov/about-nci/organization/ccg/research/structural-genomics/tcga (Accessed on: 11 February 2022).
[52] ImageCLEF/LifeCLEF-Multimedia Retrieval in CLEF. Available from: https://web.archive.org/web/ 20220301143736/https://www.imageclef.org/2017/tuberculosis (Accessed on: 3 January 2022).
[53] SCR database: Segmentation in chest radiographs. Available from: https://web.archive.org /web/20220302073253/https://www.isi.uu.nl/Research/Databases/SCR/ (Accessed on: 10 January 2022).
[54] JSRT Database. Available from: rchive.org/web/20220302073541/http://db.jsrt.or.jp/eng.php (Accessed on: 10 January 2022).
[55] Armato SG III, McLennan G, Bidaut L, *et al.* The Lung Image Database Consortium (LIDC) and Image Database Resource Initiative (IDRI): A completed reference database of lung nodules on CT scans. Med Phys 2011; 38(2): 915-31. http://dx.doi.org/10.1118/1.3528204 PMID: 21452728
[56] Setio AAA, Traverso A, de Bel T, *et al.* Validation, comparison, and combination of algorithms for automatic detection of pulmonary nodules in computed tomography images: The LUNA16 challenge. Med Image Anal 2017; 42: 1-13. http://dx.doi.org/10.1016/j.media.2017.06.015 PMID: 28732268
[57] Sahiner B, Pezeshk A, Hadjiiski LM, *et al.* Deep learning in medical imaging and radiation therapy. Med Phys 2019; 46(1): e1-e36. http://dx.doi.org/10.1002/mp.13264 PMID: 30367497
[58] Zhou X, Li C, Rahaman MM, *et al.* A comprehensive review for breast histopathology image analysis using classical and deep neural networks. IEEE Access 2020; 8: 90931-56. http://dx.doi.org/10.1109/ACCESS.2020.2993788
[59] Lee LK, Liew SC, Thong WJ. A review of image segmentation methodologies in medical image. Adv Comput Commun Eng Technol 2015; 315(1069): 80. http://dx.doi.org/10.1007/978-3-319-07674-4_99
[60] LeCun Y, Kavukcuoglu K, Farabet C. Convolutional networks and applications in vision. Proceedings of 2010 IEEE international symposium on circuits and systems. 30 May-2 June 2010; Paris, France: IEEE 253-6.
[61] Goodfellow I, Pouget-Abadie J, Mirza M, *et al.* Generative adversarial nets. Adv Neural Inf Process Syst 2014; 2014: 27.
[62] Raza K, Singh NK. A tour of unsupervised deep learning for medical image analysis. Curr Med Imaging Rev 2021; 17(9): 1059-77. http://dx.doi.org/10.2174/1573405617666210127154257 PMID: 33504314
[63] Simonyan K, Zisserman A. Very deep convolutional networks for large-scale image recognition. arXiv 2014; 2014: 14091556.
[64] Zhao T, Gao D, Wang J, Yin Z. Lung segmentation in CT images using a fully convolutional neural network with multi-instance and conditional adversary loss. 2018 IEEE 15th International Symposium on Biomedical Imaging (ISBI 2018). 24 May 2018; Washington DC, USA: IEEE; pp 505-9. http://dx.doi.org/10.1109/ISBI.2018.8363626
[65] Long J, Shelhamer E, Darrell T. Fully convolutional networks for semantic segmentation. Proceedings of the IEEE conference on computer vision and pattern recognition. Boston, MA, USA. 2015; pp. 3431-40.
[66] Ronneberger O, Fischer P, Brox T. U-Net: Convolutional networks for biomedical image segmentation. In: Navab N, Hornegger J, Wells W, Frangi A. Eds.; Medical Image Computing and Computer-Assisted Intervention – MICCAI 2015: MICCAI 2015. Lecture Notes in Computer Science, Vol. 9351. Springer, Cham. http://dx.doi.org/10.1007/978-3-319-24574-4_28
[67] Liu T, Qian B, Wang Y, Xie Q. U-Net medical image segmentation based on attention mechanism combination. Int Conf Cogn Inform Proc Appl (CIPA) 2021; 2021: 805-13. http://dx.doi.org/10.1007/978-981-16-5857-0_103
[68] Zou KH, Warfield SK, Bharatha A, *et al.* Statistical validation of image segmentation quality based on a spatial overlap index1. Acad Radiol 2004; 11(2): 178-89. http://dx.doi.org/10.1016/S1076-6332(03)00671-8 PMID: 14974593
[69] Anwar SM, Majid M, Qayyum A, Awais M, Alnowami M, Khan MK. Medical image analysis using convolutional neural networks: a review. J Med Syst 2018; 42(11): 226. http://dx.doi.org/10.1007/s10916-018-1088-1 PMID: 30298337
[70] Havaei M, Davy A, Warde-Farley D, *et al.* Brain tumor segmentation with deep neural networks. Med Image Anal 2017; 35: 18-31. http://dx.doi.org/10.1016/j.media.2016.05.004 PMID: 27310171
[71] Yuan Y, Chao M, Lo YC. Automatic skin lesion segmentation using deep fully convolutional networks with jaccard distance. IEEE Trans Med Imaging 2017; 36(9): 1876-86. http://dx.doi.org/10.1109/TMI.2017.2695227 PMID: 28436853
[72] Kumar Y, Gupta S, Singla R, Hu Y-C. A systematic review of artificial intelligence techniques in cancer prediction and diagnosis. Arch Comput Methods Eng 2021; 2021: 1-28. PMID: 34602811
[73] Feng X, Qing K, Tustison NJ, Meyer CH, Chen Q. Deep convolutional neural network for segmentation of thoracic organs-at-risk using cropped 3D images. Med Phys 2019; 46(5): 2169-80. http://dx.doi.org/10.1002/mp.13466 PMID: 30830685
[74] Zhao X, Li L, Lu W, Tan S. Tumor co-segmentation in PET/CT using multi-modality fully convolutional neural network. Phys Med Biol 2018; 64(1): 015011. http://dx.doi.org/10.1088/1361-6560/aaf44b PMID: 30523964
[75] Siegel RL, Miller KD, Fuchs HE, Jemal A. Cancer statistics, 2022. CA Cancer J Clin 2022; 72(1): 7-33. http://dx.doi.org/10.3322/caac.21708 PMID: 35020204

[76] Sheng K. Artificial intelligence in radiotherapy: a technological review. Front Med 2020; 14(4): 431-49. http://dx.doi.org/10.1007/s11684-020-0761-1 PMID: 32728877

[77] Zhang F, Wang Q, Li H. Automatic segmentation of the gross target volume in non-small cell lung cancer using a modified version of resNet. Technol Cancer Res Treat 2020; 19: 1533033820947484. http://dx.doi.org/10.1177/1533033820947484

[78] Pang S, Du A, Orgun MA, *et al.* CTumorGAN: a unified framework for automatic computed tomography tumor segmentation. Eur J Nucl Med Mol Imaging 2020; 47(10): 2248-68. http://dx.doi.org/10.1007/s00259-020-04781-3 PMID: 32222809

[79] Jiang J, Hu YC, Tyagi N, *et al.* Cross-modality (CT-MRI) prior augmented deep learning for robust lung tumor segmentation from small MR datasets. Med Phys 2019; 46(10): 4392-404. http://dx.doi.org/10.1002/mp.13695 PMID: 31274206

[80] Jiang J, Riyahi Alam S, Chen I, *et al.* Deep cross-modality (MR-CT) educed distillation learning for cone beam CT lung tumor segmentation. Med Phys 2021; 48(7): 3702-13. http://dx.doi.org/10.1002/mp.14902 PMID: 33905558

[81] Leung KH, Marashdeh W, Wray R, *et al.* A physics-guided modular deep-learning based automated framework for tumor segmentation in PET. Phys Med Biol 2020; 65(24): 245032. http://dx.doi.org/10.1088/1361-6560/ab8535 PMID: 32235059

[82] Li L, Zhao X, Lu W, Tan S. Deep learning for variational multimodality tumor segmentation in PET/CT. Neurocomputing 2020; 392: 277-95. http://dx.doi.org/10.1016/j.neucom.2018.10.099 PMID: 32773965

[83] Bi L, Fulham M, Li N, *et al.* Recurrent feature fusion learning for multi-modality pet-ct tumor segmentation. Comput Methods Programs Biomed 2021; 2021: 203106043. http://dx.doi.org/10.1016/j.cmpb.2021.106043 PMID: 33744750

[84] Fu X, Bi L, Kumar A, Fulham M, Kim J. Multimodal spatial attention module for targeting multimodal PET-CT lung tumor segmentation. IEEE J Biomed Health Inform 2021; 25(9): 3507-16. http://dx.doi.org/10.1109/JBHI.2021.3059453 PMID: 33591922

[85] Bi N, Wang J, Zhang T, *et al.* Deep learning improved clinical target volume contouring quality and efficiency for postoperative radiation therapy in non-small cell lung cancer. Front Oncol 2019; 9: 1192. http://dx.doi.org/10.3389/fonc.2019.01192 PMID: 31799181

[86] Jemaa S, Fredrickson J, Carano RAD, Nielsen T, de Crespigny A, Bengtsson T. Tumor segmentation and feature extraction from whole-body FDG-PET/CT using cascaded 2D and 3D convolutional neural networks. J Digit Imaging 2020; 33(4): 888-94. http://dx.doi.org/10.1007/s10278-020-00341-1 PMID: 32378059

[87] Jiang J, Hu YC, Liu CJ, *et al.* Multiple resolution residually connected feature streams for automatic lung tumor segmentation from CT images. IEEE Trans Med Imaging 2019; 38(1): 134-44. http://dx.doi.org/10.1109/TMI.2018.2857800 PMID: 30040632

[88] Vallières M, Freeman CR, Skamene SR, El Naqa I. A radiomics model from joint FDG-PET and MRI texture features for the prediction of lung metastases in soft-tissue sarcomas of the extremities. Phys Med Biol 2015; 60(14): 5471-96. http://dx.doi.org/10.1088/0031-9155/60/14/5471 PMID: 26119045

[89] Zhu J, Zhang J, Qiu B, Liu Y, Liu X, Chen L. Comparison of the automatic segmentation of multiple organs at risk in CT images of lung cancer between deep convolutional neural network-based and atlas-based techniques. Acta Oncol 2019; 58(2): 257-64. http://dx.doi.org/10.1080/0284186X.2018.1529421 PMID: 30398090

[90] Vesal S, Ravikumar N, Maier A. A 2D dilated residual U-Net for multi-organ segmentation in thoracic CT. arXiv 2019; 2019: 190507710.

[91] Dong X, Lei Y, Wang T, *et al.* Automatic multiorgan segmentation in thorax CT images using U-net- GAN. Med Phys 2019; 46(5): 2157-68. http://dx.doi.org/10.1002/mp.13458 PMID: 30810231

[92] He T, Hu J, Song Y, Guo J, Yi Z. Multi-task learning for the segmentation of organs at risk with label dependence. Med Image Anal 2020; 61101666 http://dx.doi.org/10.1016/j.media.2020.101666 PMID: 32062155

[93] Chen S, Zhong X, Hu S, *et al.* Automatic multi-organ segmentation in dual-energy CT (DECT) with dedicated 3D fully convolutional DECT networks. Med Phys 2020; 47(2): 552-62. http://dx.doi.org/10.1002/mp.13950 PMID: 31816095

[94] Hu Q, de F Souza LF, Holanda GB, *et al.* An effective approach for CT lung segmentation using mask region-based convolutional neural networks. Artif Intell Med 2020; 2020: 103101792. http://dx.doi.org/10.1016/j.artmed.2020.101792 PMID: 32143797

[95] van Harten LD, Noothout JM, Verhoeff JJ, Wolterink JM, Isgum I. Automatic segmentation of organs at risk in thoracic CT scans by combining 2D and 3D convolutional neural networks. SegTHOR@ ISBI 2019; 2019: 139099960.

[96] Akila Agnes S, Anitha J, Dinesh Peter J. Automatic lung segmentation in low-dose chest CT scans using convolutional deep and wide network (CDWN). Neural Comput Appl 2020; 32(20): 15845-55. http://dx.doi.org/10.1007/s00521-018-3877-3

[97] Zhang T, Yang Y, Wang J, *et al.* Comparison between atlas and convolutional neural network based automatic segmentation of multiple organs at risk in non-small cell lung cancer. Medicine (Baltimore) 2020; 99(34): e21800. http://dx.doi.org/10.1097/MD.0000000000021800 PMID: 32846816

[98] Cid YD, Del Toro OAJ, Depeursinge A, Müller H. Efficient and fully automatic segmentation of the lungs in CT volumes. VISCERAL Challenge@ ISBI 16-19 April 2015; NY, USA; pp 31-5.

[99] Lambert Z, Petitjean C, Dubray B, Kuan S. Tenth International Conference on Image Processing Theory, Tools and Applications (IPTA). 9-12 November 2020; Paris, France: IEEE 2020; pp. 1-6.

[100] Choi RY, Coyner AS, Kalpathy-Cramer J, Chiang MF, Campbell JP. Introduction to machine learning, neural networks, and deep learning. Transl Vis Sci Technol 2020; 9(2): 14-4. PMID: 32704420

[101] Winfield JM, Payne GS, deSouza NM. Functional MRI and CT biomarkers in oncology. Eur J Nucl Med Mol Imaging 2015; 42(4): 562-78. http://dx.doi.org/10.1007/s00259-014-2979-0 PMID: 25578953

[102] Fechter T, Adebahr S, Baltas D, Ben Ayed I, Desrosiers C, Dolz J. Esophagus segmentation in CT *via* 3D fully convolutional neural network and random walk. Med Phys 2017; 44(12): 6341-52. http://dx.doi.org/10.1002/mp.12593 PMID: 28940372

[103] Giovannini S, Macchi C, Liperoti R, *et al.* Association of body fat with health-related quality of life and depression in nonagenarians: The mugello study. J Am Med Dir Assoc 2019; 20(5): 564-8. http://dx.doi.org/10.1016/j.jamda.2019.01.128 PMID: 30852165

[104] Lin X, Jiao H, Pang Z, *et al.* Lung cancer and granuloma identification using a deep learning model to extract 3-dimensional radiomics features in CT imaging. Clin Lung Cancer 2021; 22(5): e756-66. http://dx.doi.org/10.1016/j.cllc.2021.02.004 PMID: 33678583

[105] Coraci D, Giovannini S, Loreti C, Fusco A, Padua L. Management of neuropathic pain: A graph theory-based presentation of literature review. Breast J 2020; 26(3): 581-2. http://dx.doi.org/10.1111/tbj.13622 PMID: 31495044